NANO: Brief Reports and Reviews
Vol. 4, No. 6 (2009) 351–358

DOI: 10.1142/S1793292009001927

World Scientific
www.worldscientific.com

FABRICATION AND MEASUREMENT OF SUSPENDED SILICON CARBIDE NANOWIRE DEVICES AND DEFLECTION

INHWA JUNG*,†
Department of Mechanical Engineering and the Texas Materials Institute
University of Texas at Austin, Austin, Texas, 78712, USA
ijung@illinois.edu

JAE-HYUN CHUNG
Department of Mechanical Engineering
University of Washington, Seattle, Washington, 98195, USA
jae71@u.washington.edu

RICHARD PINER‡, JI WON SUK§ and RODNEY S. RUOFF†,¶
Department of Mechanical Engineering and the Texas Materials Institute
University of Texas at Austin, Austin, Texas, 78712, USA
‡*r-piner@mail.utexas.edu*
§*jwsuk@mail.utexas.edu*
¶*r.ruoff@mail.utexas.edu*

Received 21 August 2009
Revised 13 October 2009

In this paper, we report the measurement of the deflection of β-SiC nanowires supported at both ends. Such wires hold promise as active elements in NEMS/MEMS devices. To ensure the stable mechanical clamping and electrical contacts between electrodes and nanowires, we have developed a method of metal deposition to improve the contacts. This method consists of multiple depositions at different angles in order to avoid the shadow effect and reduce the compressive residual stress. The improvement of the contacts was verified via SEM observation and electrical transport measurements. To suspend the nanowire, a dielectric layer underneath was removed, followed by critical point drying. The change of electrical resistance was measured when the suspended nanowires were deflected by either capillary forces arising from the surface tension or electrostatic forces.

Keywords: Suspended nanowires; microfabrication; capillary forces; deflection sensor.

1. Introduction

Suspended structures are active elements in NEMS/MEMS devices because they are deformable by bending and twisting. To fabricate suspended structures, conventional device fabrication procedures, which consist of thin film deposition,

*Present address: The Frederick Seitz Materials Research Laboratory, Room 3020, University of Illinois at Urbana-Champaign, IL 61801, USA.
†Corresponding authors.

patterning and etching, have been tried.[1–6] Recently, it has been reported that suspended structures can be made by depositing[7–14] or directly growing[10,11,15,16] nanomaterials on a substrate. A variety of materials, either synthesized or naturally existing, can be utilized in this method. However, the controlled assembly of nanomaterials onto the specified positions is challenging because the synthesis of nanomaterial relies on stochastic process from vapor phase chemicals. To solve this problem, electric fields have been applied to assemble nanomaterials onto electrodes.[8,17] An individual nanomaterial can also be handled by a manipulating stage.[18–22]

An advantage of using a synthesized nanomaterial is that its dimensional parameter, i.e., the diameter for an one-dimensional nanowire or the thickness for a two-dimensional sheet or film, can be reduced to an atomic level. This characteristic is useful for minimizing devices. The high aspect ratio structure can enhance the sensitivity to molecular adsorption and the mechanical flexibility to external forces. Electromechanical resonators made of a carbon nanotube[15] or graphene sheet[12] are outstanding examples. However, it is challenging to integrate these nanometer scale materials into reliable devices. In contrast, the material of relatively large scale is more stable and more easily handled for fabrication. A stable contact between the nanomaterials and electrodes still remains a critical challenge for nanoscale devices, which is addressed in this paper.

In our research, commercially available β-SiC nanowires are used to fabricate a suspended structure. The typical diameter of these nanowires is about a few hundred nanometers. The lengths of the nanowires vary from 1 to 100 μm.[23] Inferring from the properties of silicon carbide, it is mechanically stiff[24] and chemically inert.[25] SiC wires have been embedded in a composite to enhance the mechanical strength. A change in conductivity under stress has also been measured.[26] Therefore, this SiC nanowire is a good candidate for an electromechanical transducer. To demonstrate the electromechanical performance, the electrical and mechanical contact between the nanowire and electrodes is crucial. The challenge lies in the contact method for SiC nanowires, which is a few hundred nanometers in diameter. To resolve this problem, a metal deposition method is presented in this paper. Two consecutive evaporations of metal layers are performed with different evaporation angles in order to avoid the shadow effect and reduce the compressive stress. The improvement in the contacts is verified by a scanning electron microscope (SEM) and electric measurement. After the electrical contact, a nanowire is suspended. The suspended nanowire is bent by capillary forces arising from the surface tension electrostatic forces. This deflection is detected electronically.

2. Experimental

2.1. *Device fabrication procedure*

Figure 1(a) shows the fabrication process for SiC nanowire devices. The procedure consists of dielectric layer growth, nanowire deposition, metallization and suspension of nanowires.

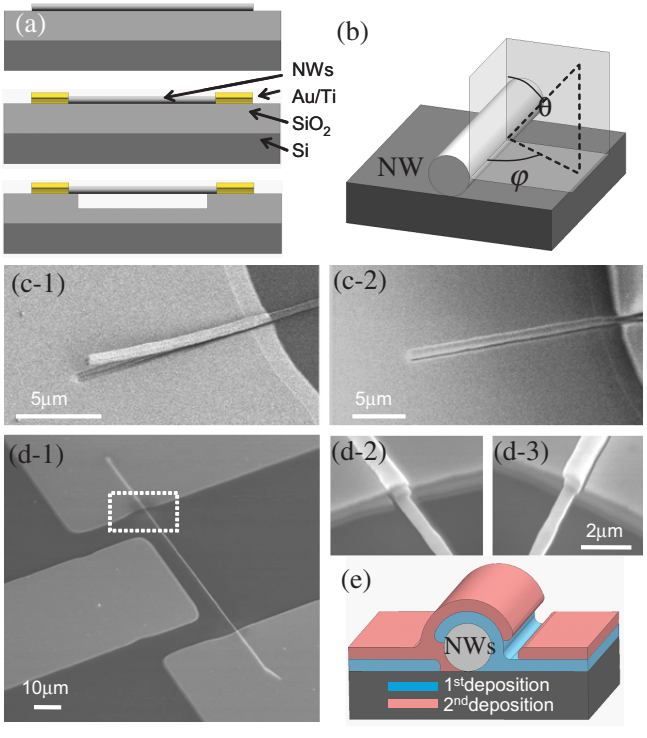

Fig. 1. Fabricating (suspended) β-SiC nanowire devices and nanowire–metal contacts. (a) Fabrication process of suspended nanowires structure: deposit nanowires onto SiO_2 on silicon (top), deposit metal layer (Au on Ti) (middle), suspend nanowires by etching SiO_2 underneath (bottom). (b) Definition of the deposition angle in spherical coordinate (θ: the zenith angle, φ: the azimuth angle). (c) Scanning electron microscope images of the contact between the metal and nanowire from previous metal deposition method: a nanowire is detached during the process (c-1), not detached during the process (c-2). (d) Images of a device by the proposed method of metal deposition: close-up images of the contact between the metal and nanowire from different view angles (d-2), (d-3). (e) A schematic of deposited metal by the proposed method.

2.1.1. *SiC nanowires*

β-SiC nanowires (from Advanced Composite Materials Corporation) were dispersed in ethanol using an ultrasonic cleaning bath. Then, nanowires were deposited on an oxide layer of a silicon substrate. From optical microscope and scanning electron microscope (SEM; Hitachi S-4500) images, lengths of the nanowire ranged from 1 μm to 100 μm and diameters ranged from 200 nm to 700 nm.

2.1.2. *Growth of silicon dioxide layer*

Silicon dioxide layer is grown on a silicon wafer by thermal oxidation method. The temperature for growth was 1100°C using an atmospheric oxidation furnace from Bruce Technologies, Inc., located in the Nanotechnology Core Facility at the University of Illinois at Chicago. Thickness of the dielectric layer was 550 ± 50 nm, but a thicker oxide film, 1200 ± 100 nm, was also grown to make devices with a higher depth of the trench (See Case 5 in Table 1). The thickness was measured by a mechanical profiler (P-1 Long Scan Profiler from Tencor). For this measurement, a rectangular open window (40 μm by 20 μm by hard-baked positive photoresist: 1818 from Shipley) was fabricated in the oxide layer. This method is also used for estimating the etch rate.

2.1.3. *Metallization*

Double metal layers (Ti/Au: 300/50 nm) were evaporated by an e-beam metal evaporator (Varian). Two different methods of metallization have been attempted. In the first method, the electric contact was made by depositing double metal layers (Ti/Au: 300/50 nm) through the rotation of a planetary system. In the second method, metal layers were formed by two consecutive evaporations at different deposition angles, which were aimed for enhancing the coverage of the deposition. The angle has two components in cylindrical coordinates: θ is the zenith angle and φ is the azimuth angle as shown in Fig. 1(b). During the deposition, φ is fixed to 90° and θ is chosen as 8° by comparing result of metal deposition from two angles (8° and 16°). For the initial run, the first layer (Ti: 150 nm) was deposited to a side of the nanowire. Subsequently, the second layer (Au/Ti: 50/150 nm) was deposited to the other side of the nanowires.

2.1.4. *Nanowire suspension*

The nanowires were suspended by etching the underlying silicon dioxide layer using a buffered oxide etchant (6:1 ratio of water/hydrofluoric acid). The etching rate was about 100 nm/min, thus the etching depth can be controlled by the etching time. To avoid the damage from the etchant, the metal electrodes and the electrode–nanowire contacts were protected by a hard-baked photoresist (baked at 140°C for 5 min). After etching, the hard-baked photoresist layer was etched away by a remover (1112A from Shipley). For the drying process, the substrates were immersed in acetone and then transferred into a critical point dryer (E3000 from Quorum Technologies) to minimize the capillary force from drying liquid (carbon dioxide).

2.2. *I–V measurement and actuation*

The current–voltage curves were measured for the fabricated devices from the probe station. A DC bias was applied by a voltage source (HP 6612C), then the current was measured and averaged by a picoammeter (Keithley 6485). The suspended nanowires were actuated by an electrostatic potential between the nanowire and the electrode. The electrode for the actuation is patterned adjacent to the nanowire as shown in Fig. 1(d-1). The distance between the nanowire and the actuation electrode is 5 μm. For the electrostatic potential, either a DC (0–60 V by Agilent 6544A) or a biased AC (10 V peak to peak by Agilent 33120A) was applied. The deflection was detected by measuring the change of the current when a constant voltage was applied to the nanowire–electrode circuitry.

3. Result and Discussion

SEM images in Fig. 1(c) show two cases of contact between nanowires and metal electrodes. The electrical contact was made by depositing double metal layers through the rotation of a planetary system. The planetary system was designed for the uniform deposition of metal layers by continuously changing the deposition angle. However, the contact could not be made because the nanowires were detached during the deposition (Fig. 1(c-1)). The partial detachment was caused by the compressive stress of a deposited film during the evaporation. The four samples out of the eight samples were damaged by the detachment. Even for the nanowires of

the successful samples (Fig. 1(c-2)), the mechanical clamping was apparently not successful owing to the shadow effect.[27] The rotation of the planetary prohibited the metal layer from deposition to the shadowed area masked by the nanowire.

The electrical contact could be greatly improved by the proposed method of metallization (For details of the fabrication method, see experimental section). The SEM images of contact by the improved method are shown in Fig. 1(d). As shown in figure, the coverage of deposition was greatly enhanced. The metal layer deposited by the first run could hold a nanowire on an oxide layer. Subsequently, the metal layer formed by the second run could cover the area that was shadowed at the first run (See illustration of Fig. 1(e)). In addition, the method avoids nanowires being partially detached. Out of the twenty samples, all the devices showed a stable coverage without partial detachment.

The improvement of the contact was also validated by electrical measurement. Current–voltage curves of three samples fabricated by the double evaporations are shown in Fig. 2(a). Because the diameters of the nanowires and the distance between the source and drain electrodes are changed, the slopes of the curves vary. However, when the resistivity of the nanowires was calculated from the measurement at 10 V, the variation was less than 1%. The average value and the standard deviation of the resistivity were $4.6 \times 10^{-2} \Omega \cdot \mathrm{m}$ and $7.0 \times 10^{-4} \Omega \cdot \mathrm{m}$, respectively. This value was computed by the equation: $\rho = (V/I - R_C)A/L$, where V is the voltage, I is the current, A is the cross-sectional area of a nanowire, and L is the distance between the source and drain electrodes. R_C is

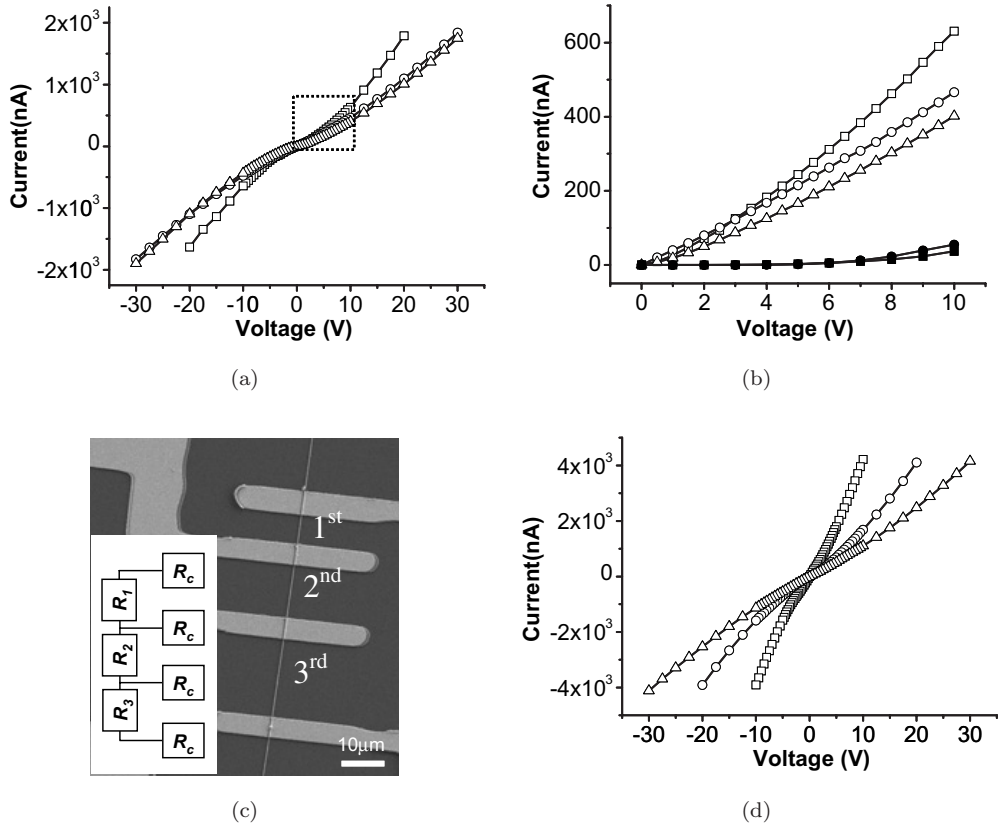

Fig. 2. Electrical transport measurement on SiC nanowire devices. (a) I–V curves for samples made by the improved metal deposition method: average diameter is 475 nm and electrode distance is 40 μm (□), average diameter is 512.5 nm and electrode distance is 60 μm (◯), average diameter is 498 nm and electrode distance is 60 μm (Δ). (b) Comparison of I–V curves for samples from two metal deposition methods: average diameter is 428.4 nm and electrode distance is 80 μm (■), average diameter is 457 nm and electrode distance is 100 μm (•) (Note: Three cases in dotted box of Fig. 2(a) are re-plotted for comparison). (c) SEM image of a nanowire device with four electrodes with increasing electrode distances (The inset is a simplified schematic for material resistance of each segment (R_1, R_2, R_3) and contact resistance (R_C)). (d) I–V curves from each segment of a nanowire: average diameter is 279 nm and electrode distance is 6.8 μm (□), average diameter is 269 nm and electrode distance is 12.6 μm (◯), average diameter is 267 nm and electrode distance is 18.5 μm (Δ).

the contact resistance, which is assumed negligible compared to the material resistance ($V/I - R_C$). Current–voltage curves for two samples prepared with a simple deposition method were measured (Fig. 2(b)).

Assuming negligible effect of contact resistance, the values of resistivity were estimated as 0.4 and 1.0 $\Omega \cdot$ m, which were significantly higher than the above cases. Consequently, the contact resistance in this case cannot be ignored.

The effect of the contact resistance could be investigated further by measuring I–V characteristics on the same nanowire. For this measurement, four electrodes are patterned on the same nanowire and the distances between each electrode are controlled roughly as 1:2:3 (see Fig. 2(c)). The current–voltage curves of each segment are shown in Fig. 2(d). Although the curves are nonlinear, the slopes are proportional to the distance between each electrode. This measurement result implies that the measurement mainly depends on properties which are proportional to the length of the material (R_1, R_2, R_3). The measured resistance is negligibly affected by contact resistances (R_C), which is independent of the length of the material (inset of Fig. 2(c)).

Apart from the above approach, the improvement of the contact can also be validated by evaluating the noise in the electric current ratio ($\Delta I/I$) at a fixed voltage bias (10 V). This measurement is important because the change of resistance is detectable as the ratio increases. The ratio was reduced from $\sim 1\%$ to $\sim 10^{-3}\%$ by the improvement. To suspend the nanowires, the silicon dioxide layer under a nanowire was removed by a wet etching process (For details of the fabrication method, see experimental section). Nanowires could be successfully suspended using a critical point dryer, which reduced capillary forces (Fig. 3(a-1)). Without the critical point dryer, the nanowires were pulled and collapsed to the bottom of the trench due to capillary forces arising from the surface tension from the drying liquid (Fig. 3(a-2)). However, the use of a critical point dryer did not guaranteed the successful suspension in all cases. In these cases, it is speculated that the applied force due to the surface tension applied in the critical dryer may be above the force required to pull down the nanowire.

The pull-down force depends on geometric parameters of suspended nanowire structure (Fig. 3(b)) and the elastic properties of the nanowire. *Euler–Bernoulli* beam theory was used

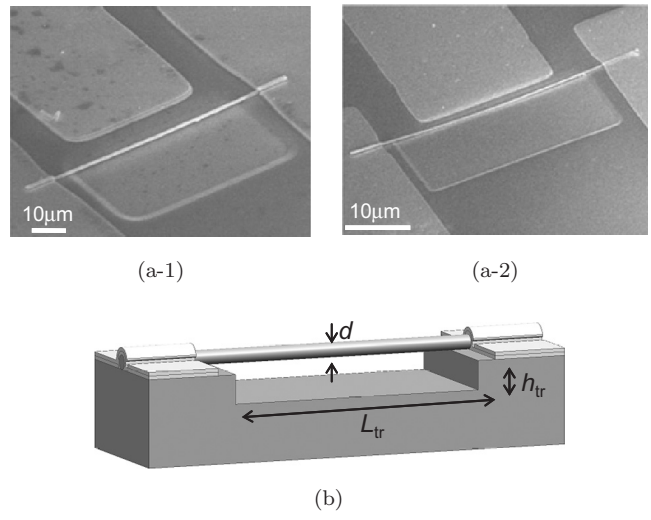

Fig. 3. Suspension of nanowires. (a) SEM images of a nanowire structure after etching underneath SiO_2: a nanowire successfully suspended by the use of critical point dryer (a-1), a nanowire pulled down due to the capillary forces arising from the surface tension of the drying liquid (a-2). (b) Geometric parameters for calculating pull-down forces: diameter of nanowires (d), length of trenches (L_{tr}) and height of trenches (h_{tr}).

to determine the force. Assuming an uniformly distributed load (ω) over the beam, the beam deflection at the center (u) is expressed as this: $u = (\omega L^4)/(384EI)$, where L is the beam length, E is the elastic modulus and I is the area moment of inertia ($\pi d^4/64$, assuming that the cross-section of the nanowire is circular). Presumably, pull-down behavior occurs when the deflection is equal to the trench depth (h), therefore the pull-down force (F) can be determined by modifying the equation above and expressed as follows: $F = 384EIh/L^3$. Elastic modulus (E) can be estimated from vibrating SiC nanowire with one end fixed, the result is in reasonable range comparing with the reported result from Dicalro.[24]

When the elastic modulus is assumed from the reported value for SiC fiber (414 ± 9 GPa), the pull-down forces of five samples are compared with the results of suspension and are shown in Table 1. From this table, the capillary force in the critical point dryer is estimated in the range between 0.4 and 0.8 μN.

These suspended nanowire systems, except for some rigid cases such as Case 5 in Table 1, are deflected and the relevant change in electrical conductivity is measured. The change of electrical conductivity of the material under stress has been previously reported for silicon carbide whiskers

Table 1. Structural parameters of nanowire structures and the results of suspension.

	Case 1	Case 2	Case 3	Case 4	Case 5
Wire diameter (nm)	348	307	360	507	707
Trench length (μm)	40	40	40	40	40
Trench depth (nm)	200	400	400	400	1000
Pull down force (μN)	0.35	0.42	0.79	3.1	29.4
Suspension result	not suspended	not suspended	suspended	suspended	suspended

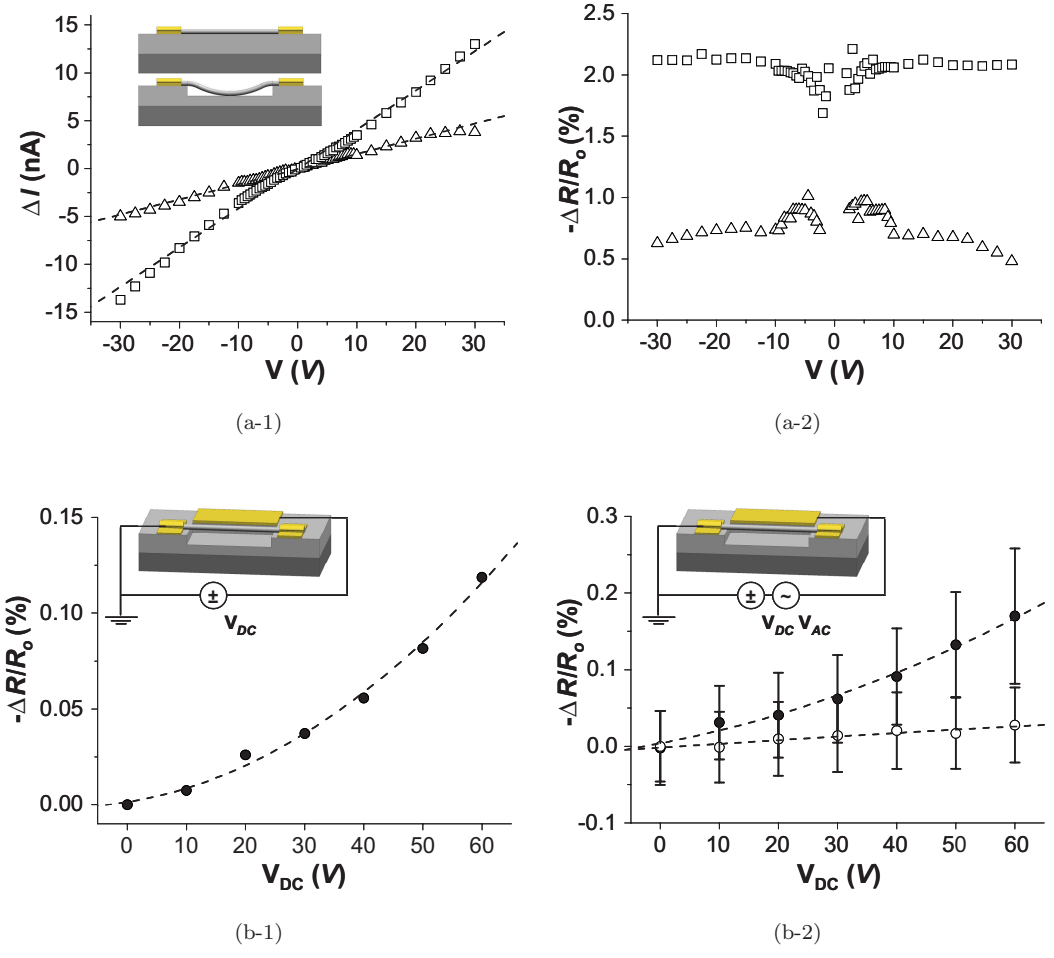

Fig. 4. Detecting deflection of suspended nanowires (a-1). Change in electric current of pull-down nanowire ($\Delta I = I$ (after pull-down) — I (before pull-down), a schematic of nanowire deflection is shown as a inset): (□) height of trench is 400 nm, nanowire diameter is 307 nm and electrodes distance is 40 μm, (Δ) height of trench is 200 nm, nanowire diameter is 348 nm and electrodes distance is 40 μm. (a-2) Decreases in resistances. (b-1) Decrease in resistance of a suspended structure with static field (V_{DC} only): (•) nanowire diameter is 360 nm and electrodes distance is 40 μm. (b-2) Decrease in resistance with dynamic field (V_{AC} (10 Vpp, 0.05 Hz) + V_{DC}): (•) the suspended structure (nanowire diameter is 360 nm and electrodes distance is 40 μm) and (◯) the pulled-down structure (nanowire diameter is 307 nm and electrodes distance is 40 μm).

embedded in composites.[26] In our case, changes in electrical conductivity of deliberately pulled-down nanowire system are measured (see inset of Fig. 4(a-1)). As a result, the electric current increased for both cases: one is 400 nm as a depth of trench (open rectangle) and the other is 200 nm (open triangle) (Fig. 4(a-1)).

This increase of electric current is related to the decrease in electrical resistance (Fig. 4(a-2)), which is proportional to the depth of the trench. For

the case where the depth of the trench is 400 nm, the decrease of resistance was $\sim 2\%$ and for the 200 nm case, resistance decreased $\sim 0.5\%$. However, the suspended nanowire can be deflected in a more controllable way by applying an electrostatic field. In this case, the deflection can be observed by an optical microscope. Either DC only or biased AC field is applied between the source and the actuation electrode. From this experiment, we measured the ratio between ΔR and R_0. $(-\Delta R/R_0)$, where R_0 is the measured resistance without an electrical field and ΔR is the difference between the instantaneous resistance (R') and R_0 $(\Delta R = R' - R_0)$. As shown in Fig. 4(b-1), the decrease of electrical resistance becomes larger when the DC field (or potential) increases. This decrease of electrical resistance is measured again when an AC potential ($10\,V_{\text{pp}}$, 0.05 Hz) is added to DC potential (Fig. 4(b-2)). It should be noted that the decrease of electrical resistance for a nonsuspended nanowire is smaller than the suspended case. From this observation, it is speculated that suspended nanowires are significantly deflected, which enhances the electrical conductivity of the system.

4. Conclusion

The contact between the metal electrode and nanowire is greatly improved by our method of metal deposition, which could be verified from a series of electrical transport measurements. By observing the pull-down of nanowires, capillary forces applied to the nanowire arising from the surface tension in the critical point dryer can be estimated, which is useful for successful suspension of nanowires. The suspended nanowire structures are deflected by capillary forces arising from the surface tension or electrostatic forces. Electrical resistance of the system, which includes nanowire, electrodes and contacts, decreased as the nanowires were deflected. The structure can be useful for investigating the correlation between electrical and mechanical properties of the material.

Acknowledgments

We acknowledge support from the National Science Foundation (CMS-0510212), the Naval Research Laboratory (No. N00173-04-2-C003) and the DARPA Center on Nanoscale Science and Technology for Integrated Micro/Nano-Electromechanical Transducers (iMINT) (Award No: HR0011-06-1-0048).

References

1. A. N. Cleland and M. L. Roukes *Nature* **392**, 160 (1998).
2. S. Evoy, D. W. Carr, L. Sekaric, A. Olkhovets, J. M. Parpia and H. G. Craighead, *J. Appl. Phys.* **86**, 6072 (1999).
3. H. G. Craighead, *Science* **290**, 1532 (2000).
4. B. Ilic, H. G. Craighead, S. Krylov, W. Senaratne, C. Ober and P. Neuzil, *J. Appl. Phys.* **95**, 3694 (2004).
5. L. Sekaric, M. Zalalutdinov, R. B. Bhiladvala, A. T. Zehnder, J. M. Parpia and H. G. Craighead, *Appl. Phys. Lett.* **81**, 2641 (2002).
6. L. Sekaric, M. Zalalutdinov, S. W. Turner, A. T. Zehnder, J. M. Parpia and H. G. Craighead, *Appl. Phys. Lett.* **80**, 3617 (2002).
7. M. F. Yu, T. Kowalewski and R. S. Ruoff, *Phys. Rev. Lett.* **85**, 1456 (2000).
8. S. N. Lu, J. Chung and R. S. Ruoff, *Nanotechnoloy* **16**, 1765 (2005).
9. L. Shi, Q. Hao, C. H. Yu, N. Mingo, X. Y. Kong and Z. L. Wang, *Appl. Phys. Lett.* **84**, 2638 (2004).
10. L. Shi, D. Y. Li, C. H. Yu, W. Y. Jang, D. Kim, Z. Yao, P. Kim and A. Majumdar, *J. Heat Trans-T. ASME* **125**, 881 (2003).
11. L. Shi, C. H. Yu and J. H. Zhou, *J. Phys. Chem. B* **109**, 22102 (2005).
12. J. S. Bunch, A. M. van der Zande, S. S. Verbridge, I. W. Frank, D. M. Tanenbaum, J. M. Parpia, H. G. Craighead and P. L. McEuen, *Science* **315**, 490 (2007).
13. A. A. Balandin, S. Ghosh, W. Z. Bao, I. Calizo, D. Teweldebrhan, F. Miao and C. N. Lau, *Nano Lett.* **8**, 902 (2008).
14. I. W. Frank, D. M. Tanenbaum, A. M. Van der Zande and P. L. McEuen, *J. Vac. Sci. Technol. B* **25**, 2558 (2007).
15. V. Sazonova, Y. Yaish, H. Ustunel, D. Roundy, T. A. Arias and P. L. McEuen, *Nature* **431**, 284 (2004).
16. C. H. Yu, L. Shi, Z. Yao, D. Y. Li and A. Majumdar, *Nano Lett.* **5**, 1842 (2005).
17. J. H. Chung, K. H. Lee, J. H. Lee and R. S. Ruoff, *Langmuir* **20**, 3011 (2004).
18. X. Q. Chen, S. L. Zhang, D. A. Dikin, W. Ding, R. S. Ruoff, L. J. Pan and Y. Nakayama, *Nano Lett.* **3**, 1299 (2003).
19. W. Ding, L. Calabri, K. M. Kohlhaas, X. Chen, D. A. Dikin and R. S. Ruoff, *Exp. Mech.* **47**, 25 (2007).
20. W. Q. Ding, L. Calabri, X. Q. Chen, K. M. Kohhaas and R. S. Ruoff, *Compos. Sci. Technol.* **66**, 1112 (2006).

21. M. F. Yu, B. S. Files, S. Arepalli and R. S. Ruoff, *Phys. Rev. Lett.* **84**, 5552 (2000).
22. M. F. Yu, O. Lourie, M. J. Dyer, K. Moloni, T. F. Kelly and R. S. Ruoff, *Science* **287**, 637 (2000).
23. K. Oh, J. H. Chung, J. J. Riley, Y. L. Liu and W. K. Liu, *Langmuir* **23**, 11932 (2007).
24. J. A. Dicarlo, *J. Mater. Sci.* **21**, 217 (1986).
25. D. Zhuang and J. H. Edgar, *Mater. Sci. Eng. R* **48**, 1 (2005).
26. S. K. Wang and D. D. L. Chung, *Smart Mater. Struct.* **6**, 199 (1997).
27. J. G. Bai, C. L. Chang, J. H. Chung and K. H. Lee, *Nanotechnology* **18**, 8 (2007).